

# DETECTION OF INDIVIDUAL DOPANTS IN SINGLE-ELECTRON DEVICES - A STUDY BY KFM OBSERVATION AND SIMULATION

Maciej Ligowski, Daniel Moraru, Anwar Miftahul, Juli Cha Tarido, Takeshi Mizuno, Michiharu Tabbe, Ryszard Jabłoński

## Abstract:

Single electron devices (SEDs) are candidates to become a keystone of future electronics. They are very attractive due to low power consumption, small size or high operating speed. It is even possible to assure compatibility with present CMOS technology when natural potential fluctuations introduced by dopant atoms are used to create quantum dots (QD). However, the main problem of this approach is due to the randomness of dopant distribution which is characteristic for conventional doping techniques. This leads to scattered characteristics of the devices, which precludes from using them in the circuits. In these work we approach the problem of correlating the distribution of QD's with the device characteristics. For that, we investigate with a Kelvin probe force microscope (KFM) the surface potential of Si nanodevice channel in order to understand the potential landscape. Results reveal the features ascribable to individual dopants. These findings are supported also by simulation results.

**Keywords:** single dopant, Kelvin Probe Force Microscope, single-electron transfer.

## 1. Introduction

Single-electron transport through individual impurity atoms has attracted wide interest for applications such as quantum computing [1] or single-electron transfer schemes [2], [3]. So far, researches focused either on heavily-doped field-effect transistors (FETs) [4] or on isolated impurities in nanoscale channels [5], [6]. In both cases, however, natural potential fluctuations caused by ionized dopant atoms were utilized. This is a very attractive idea since it assures compatibility with present CMOS technology. In Fig. 1(a) we can observe the schematic view of the device. The source and the drain are connected by a doped nanowire which is so small that it consists of only a few dopant atoms. These dopants introduce natural potential fluctuations (seen in Fig. 1(c)) which under appropriate biasing conditions create quantum dots separated by tunnel barriers (see Fig. 1(d)). Electrons can be accumulated in these quantum dots in the proximity of the dopants. However, since the dots are very small they can accumulate only one or few electrons. Therefore electrons can tunnel through the tunnel barriers to enter the dot only if previous electrons have been already removed. This phenomenon is known as Coulomb blockade and it is a principle of single electron tunneling operation [7].

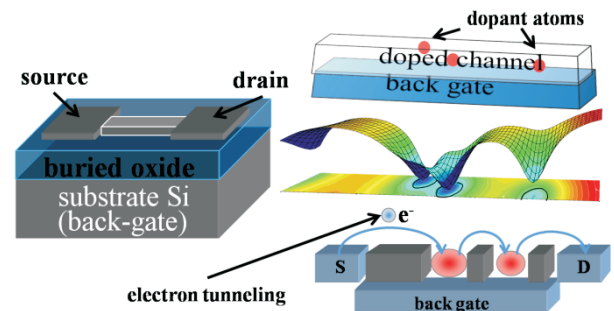


Fig.1. Single electron tunneling in Si nanodevice; (a) device structure; (b) Nanodevice channel - doped Si nanowire; (c) surface potential profile of the channel; (d) effective structure of quantum dots and tunneling barriers in the device.

It is natural to assume that in above described systems the distribution of dopant atoms in the channel influences the device parameters and therefore is of great importance. Unfortunately, when conventional doping techniques are used, only a random dopant distribution can be achieved. Therefore, monitoring the dopant distribution is a necessary step towards constructing a standardized SED with predictable characteristics.

## 2. The resolution limits of KFM

Kelvin Probe Force Microscope (KFM) [8] seems to be the most appropriate tool for dopant distribution monitoring due to its high resolution and sensitivity [9]. There are admittedly several reports of shallow dopant profile or carrier concentration measurements by scanning tunneling microscopy (STM) or scanning capacitance microscopy (SCM). However, STM techniques, which are mainly used so far, allow investigating only several top-most layers [10]. SCM, on the other hand, in principle is not suitable tool for single dopant detection and thus achieved results are of much lower resolution [11].

In KFM, surface potential map is obtained by measuring the potential offset between a probe tip and a surface. This offset causes an electrostatic force:

$$F = \frac{1}{2} \frac{\partial C}{\partial z} V^2$$

where total potential offset is given by

$$V = V_{CPD} - (V_{DC} + V_{AC} \sin \omega t)$$

The  $V_{CPD}$  is the measured contact potential difference, while  $V_{AC}$  and  $V_{DC}$  are the voltages applied for the measurement purpose. As a result of applying an AC

voltage the cantilever vibrates with the frequency  $f_0$ . When surface potential changes it changes the electrostatic force, which changes a fundamental resonant frequency according to the equation [12]:

$$f_0' = \frac{1}{2\pi} \sqrt{\frac{k - \frac{\partial F}{\partial z}}{m^*}} \approx f_0 \left(1 - \frac{1}{2k} \frac{\partial F}{\partial z}\right)$$

The  $f_0$  is a primary oscillation frequency,  $k$  is a spring constant,  $m^*$  is an effective mass and  $\partial F/\partial z$  is a force gradient. According to Zerweck *et al.* even as small as 5mV potential difference can be detected. For this signal still a frequency shift can be resolved [12].

In practical solutions, however, this high resolution is decreased by the electron screening effect. This well known phenomenon leads to the reduction of the local surface potential fluctuations and thus precludes from detecting individual dopant atoms. To overcome this problem, we propose a low temperature measurement system. According to the Fermi-Dirac distribution the probability that the electron occupies the electronic state with energy  $E$  is given by  $F(E)$ :

$$F(E) = \frac{1}{1 + e^{(E-E_F)/kT}}$$

where  $k$  is the Boltzmann constant,  $T$  is the temperature in Kelvin and  $E_F$  is the Fermi level. It can be noticed that at low temperatures the number of free carriers changes abruptly around Fermi level, which means that they can be easily depleted. On the contrary, at room temperature the change is smoothed and screening occurs.

### 3. KFM observations of individual dopant atoms

In this research we utilized KFM to visualize the potential profile of the doped Si layer. For that purpose a thin silicon-on-insulator field-effect transistor (SOI-FET) without the top gate was investigated by KFM at low temperature (13K). The substrate, which was used as a gate, was a boron doped p-Si ( $1 \times 10^{18} \text{ cm}^{-3}$ ) and the whole top Si region was doped with phosphorus ( $5 \times 10^{17} \text{ cm}^{-3}$ ). Both source and drain were grounded, while back gate voltage ( $V_g$ ) was set to -3V to deplete free carriers from the channel. The resultant KFM electronic potential image with the corresponding topography profile in the inset are presented in Fig. 2(a), while the simplified measurement setup is shown in Fig. 2(b).

Local potential fluctuations induced by randomly distributed dopant atoms can be observed in the channel surface potential. In Fig. 2(c) we can see hypothetical shape of potential well induced by one donor placed at the surface. Fig. 2(d)-(f) show profiles of chosen potential wells observed in KFM image which are ascribed to individual dopants. The size and shape of observed features match with expected phosphorus ion induced fluctuations. The circular shape of the potential dips suggests the point charge. To compare their size we refer to the diameter of the potential well 15 mV above its bottom. The lateral diameter in the range of 5-10 nm is in a good agreement to the Bohr radius of phosphorus in silicon ( $\approx 3 \text{ nm}$ ) [13]. Moreover potential difference of 25 mV seems to reflect potential well, induced by a single phosphorus

atom, reduced by screening and distance dependence. We exclude interface trapped charges or surface charge influence, since similar potential fluctuations cannot be observed in the buried oxide (BOX) region. It can be also noticed that the local potential maxima are close to the value of 0 V. This corresponds to the fact that during all the measurements the source and drain were grounded and Fermi level of the top Si layer remained at ground level. Furthermore, we conclude that the channel was partially ionized and hence conductive. As it can also be seen, the potential landscape consists of regions with lower potential (quantum dots) separated by a regions with higher potential (barriers). This image lets us assume that in the case of very thin and narrow channels a one dimensional quantum dot array can be formed.

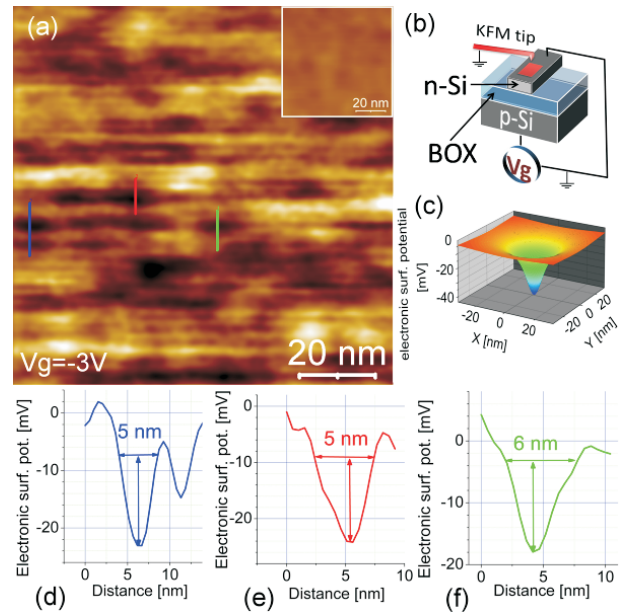


Fig. 2. (a) Surface potential map of the channel area obtained by KFM at 13K (corresponding topography profile in the inset, z-range 10nm); (b) Measurement setup and structure of back-gated SOI-FET device; (c) Surface potential dip induced by single donor atom; (d)-(f) The profiles of local potential fluctuation induced by individual phosphorus atoms measured by KFM.

To prove the results, further examination of dopant-induced potential fluctuations was performed. This time a boron-doped acceptor-type sample was investigated. The surface potential of  $1 \mu\text{m}$  thick p-Si ( $1 \times 10^{16} \text{ cm}^{-3}$ ) epitaxial layer (epi-layer) placed on p-Si ( $1 \times 10^{18} \text{ cm}^{-3}$ ) substrate was investigated by KFM at 13K. Figure 3(a) shows the resultant KFM electronic surface potential map and the topography profile in the inset. The measurement setup and sample structure can be observed in Fig. 3(b). Opposite sign of detected potential fluctuations for a p-Si epi-layer in comparison to the previous sample (n-Si channel SOI-FET) can be noticed in Fig. 3(c). Furthermore, as the doping concentration of a p-Si epi-layer is in the range of  $1 \times 10^{16} \text{ cm}^{-3}$  and assumed depth sensitivity of the KFM is 20nm, we expect to have 1 or 2 dopants visible in the measured area of  $75 \times 75 \text{ nm}^2$ . This number can vary due to random distribution and local ionization ratio of acceptors. It can be noticed, however, that for low doped

p-Si epi-layer, most of the surface potential is flat and only two ionized acceptors are clearly visible, while for n-type channel, as dopant concentration is much higher, the whole surface potential is modulated by the donor ions and remains non-uniform in the entire measured area.

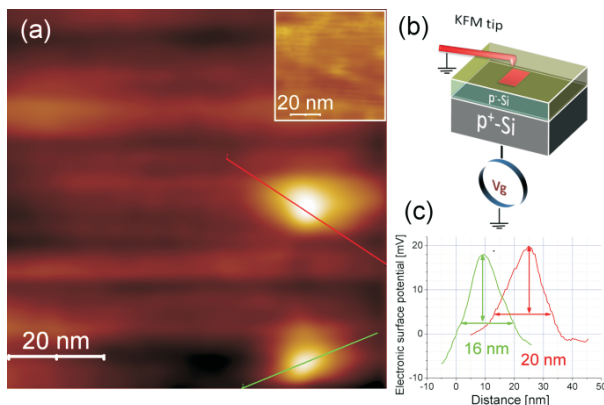


Fig. 3. (a) Surface potential map obtained by KFM at 13K, topography profile in the inset ( $z$ -range 10nm); (b) Measurement setup and structure of boron doped p-Si sample; (c) Local potential fluctuation profiles induced by individual boron atoms.

#### 4. Surface potential simulations

For comparison with experimental data, a simple simulation of surface potential was performed. In this simulation the dopants were randomly placed in a  $200 \times 200 \times 200$  nm cubic volume with the concentration of  $1 \times 10^{18} \text{ cm}^{-3}$ . Next, the potential superimposing the Coulombic potentials of all the donors introduced into the mesh was calculated in every point of the cubic mesh [13]. The obtained top-most layer (surface) potential is drawn in Fig. 3(a), while Fig. 3(b) shows the schematic view of simulated structure.

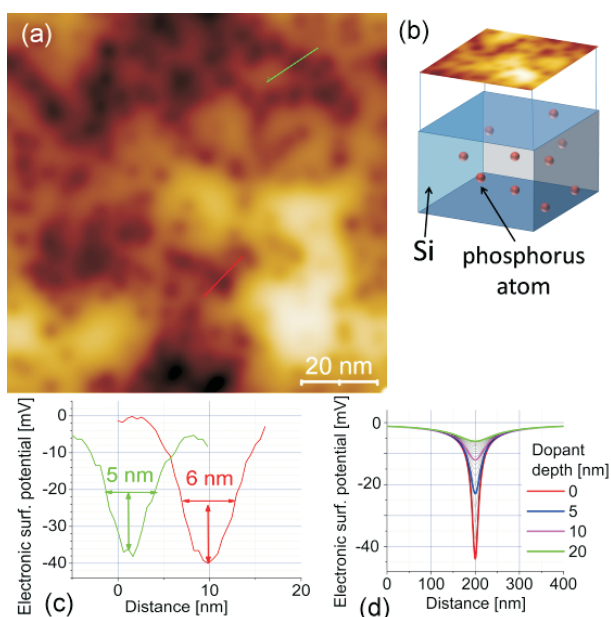


Fig. 4. (a) Surface potential map of the Si block obtained by simulation; (b) Schematic view of a simulated structure; (c) Local potential fluctuation profiles induced by individual dopant atoms or clusters; (d) The dependence between donor depth and corresponding surface potential.

There is a good correspondence between the KFM results shown in Fig. 2(a) and the simulation results shown in Fig. 3(a). It is clear that features ascribable to point charges can be distinguished in the surface potential although smooth potential changes modulated by clusters of donors can be seen as well. The diameter and shape of potential fluctuations induced by individual dopants are shown in Fig. 3(c). It can be noticed, however, that some point charges visible in the image seem to introduce shallower potential dips. To explain this discrepancy we simulated the dependence between the surface potential introduced by a single dopant and the depth on which the dopant is placed, as shown in Fig. 3(d).

#### 5. Conclusions

Recently improved capabilities of LT-KFM open an opportunity to directly observe dopant induced potential fluctuations at the surface of MOSFETs under operation. So far, no appropriate method for direct detection dopant atom positions in MOSFET has been proposed. Using LT-KFM we have detected the individual dopant atoms in thin SOI layer. These findings suggest that LT-KFM may become the best tool for precise dopant position mapping, which is crucial for future nanodevices [14]. By studying the surface potential (basing on KFM and simulation results) it may be possible to obtain an optimum shape of the device channel. Our goal is to study the correlation between number of dopant-induced QDs and electrical characteristics of short or long channel devices.

#### ACKNOWLEDGMENTS

The authors thank D. Nagata, S. Miki, R. Nakamura for support in experiments, and H. Ikeda for discussions. This work was partially supported by Grants-in-Aid for Scientific Research (16106006 and 18063010) from the Ministry of Education, Culture, Sports, Science, and Technology of Japan.

#### AUTHORS

**Maciej Ligowski\***, **Ryszard Jablonski** - Warsaw University of Technology, Division of Sensors and Measuring Systems, A. Boboli 8, Warsaw 02-525, Poland. E-mail: maciej@ligowski.com.

**Maciej Ligowski\***, **Daniel Moraru**, **Anwar Miftahul**, **Juli Cha Tarido**, **Takeshi Mizuno**, **Michiharu Tabe** - Shizuoka University, Research Institute of Electronics, Johoku 3-5-1, 432-8011 Hamamatsu, Japan.

\* Corresponding author

#### References

- [1] Kane B.E., "A Silicon Based Nuclear Spin Quantum Computer", *Nature* (London), vol. 393, 1998, pp. 133.
- [2] Moraru D., Ono Y., Inokawa H., Tabe M., "Quantized electron transfer through random multiple tunnel junctions in phosphorus-doped silicon nanowires", *Phys. Rev. B*, vol. 76, 2007, p. 075332.
- [3] Yokoi K., Moraru D., Ligowski M., Tabe M., "Single-Gated Single-Electron Transfer in Nonuniform Arrays of Quantum Dots", *Jpn. J. Appl. Phys.*, vol. 48, 2009, p. 024503.
- [4] Smith R.A., Ahmed H., "Gate controlled Coulomb bloc-

- kade effects in the conduction of a silicon quantum wire", *J. Appl. Phys.*, vol. 81, 1996, p. 2699.
- [5] Ono Y., *et al.*, "Conductance modulation by individual acceptors in Si nanoscale field-effect transistors", *Appl. Phys. Lett.*, vol. 90, 2007, p. 102106.
- [6] Sellier H., *et al.*, "Transport Spectroscopy of a Single Dopant in a Gated Silicon Nanowire", *Phys. Rev. Lett.*, vol. 97, 2006, p. 206805.
- [7] Averin D.V., Likharev K.K., in "Single charge tunneling", ed. Grabert H. and Devoret M., Plenum, New York, 1992, p. 311.
- [8] Nonnenmacher M., *et al.*, "Kelvin probe force microscopy", *Appl. Phys. Lett.*, vol. 58, 1991, p. 2921.
- [9] Ligowski M., Moraru D., Anwar M., Mizuno T., Jablonski R., Tabe M., "Observation of individual dopants in a thin silicon layer by low temperature Kelvin probe force microscope", *Appl. Phys. Lett.*, vol. 93, no. 14, 2008, p. 142101.
- [10] Nishizawa M., *et al.*, "Simultaneous measurement of potential and dopant atom distributions on wet-prepared Si(111):H surfaces by scanning tunneling microscopy", *Appl. Phys. Lett.*, vol. 90, 2007, pp. 122118.
- [11] Goragot W., Takai M., "Measurement of Shallow Dopant Profile Using Scanning Capacitance Microscopy", *Jpn. J. Appl. Phys.*, vol. 43, 2004, p. 3990.
- [12] Evans G.J., Mizuta H., Ahmed H., "Modelling of Structural and Threshold Voltage Characteristics of Randomly Doped Silicon Nanowires in the Coulomb-Blockade Regime", *Jpn. J. Appl. Phys.*, vol. 40, 2001, p. 5837.
- [13] Zerweck U., Loppacher C., Otto T., Grafström S., and L. M. Eng.
- [14] Moraru D., Ligowski M., Yokoi K., Mizuno T., Tabe M., *Appl. Phys. Exp.*, vol. 2, 2009, pp. 071201.